Biophysical Journal
Article

Biophysical Society

Miscibility Transition Temperature Scales with Growth Temperature in a Zebrafish Cell Line

Margaret Burns,[1] Kathleen Wisser,[1] Jing Wu,[1] Ilya Levental,[2] and Sarah L. Veatch[1,*]
[1]Department of Biophysics, University of Michigan, Ann Arbor, Michigan and [2]Department of Integrative Biology and Pharmacology, University of Texas Health Science Center, Houston, Texas

ABSTRACT Cells can alter the lipid content of their plasma membranes upon changes in their environment to maintain and adjust membrane function. Recent work suggests that some membrane functions arise because cellular plasma membranes are poised close to a miscibility transition under growth conditions. Here we report experiments utilizing giant plasma membrane vesicles (GPMVs) to explore how membrane transition temperature varies with growth temperature in a zebrafish cell line (ZF4) that can be adapted for growth between 20 and 32°C. We find that GPMV transition temperatures adjust to be 16.7 ± 1.2°C below growth temperature for four growth temperatures investigated and that adjustment occurs over roughly 2 days when temperature is abruptly lowered from 28 to 20°C. We also find that GPMVs have slightly different lipidomes when isolated from cells adapted for growth at 28 and 20°C. Similar to past work in vesicles derived from mammalian cells, fluctuating domains are observed in ZF4-derived GPMVs, consistent with their having critical membrane compositions. Taken together, these experimental results suggest that cells in culture biologically tune their membrane composition in a way that maintains specific proximity to a critical miscibility transition.

INTRODUCTION

It is well established that cells alter their lipid content in response to their environment. For example, bacteria and higher organisms change their membrane composition and physical properties when grown at different temperatures (1–8); yeast alter their lipid content to counteract the membrane fluidizing effects of ethanol produced during fermentation (9–11); and mammalian cells adjust their lipids during the cell cycle (12–15), when undergoing differentiation (16,17), and in response to stress or disease (18–20). The physical properties of cell membranes are primarily dictated by their complex lipid and protein compositions and facilitate many cellular functions. In this context, it is expected that cells will adjust their plasma membrane lipid composition to maintain or manipulate these properties as cells adjust to living in new environments or when they take on new functional roles. It has long been appreciated that cells adjust membrane lipids to retain a robust, fluid, and flexible barrier at the cell periphery (21–24). Other authors have argued that cells tune their membrane composition to allow for greater flexibility of the membrane matrix (25,26), or consistent membrane curvature (27). Past work in mostly mammalian cell membranes also argues that cells biochemically tune their plasma membrane composition to maintain a specific level of lipid-mediated lateral heterogeneity (28–30), which cells use to influence the organization and associations of cell surface proteins. The experiments described here provide further support for this last hypothesis.

Plasma membranes isolated from live cells experience a miscibility transition below growth temperature (31). These giant plasma membrane vesicles (GPMVs) present a single liquid phase at elevated temperatures but form coexisting liquid-ordered and liquid-disordered phases at low temperatures. Individual vesicles reversibly transition between these two states at the miscibility transition temperature or T_{mix}. The T_{mix} values measured for GPMVs isolated from mammalian cells typically range between 0 and 25°C, depending on numerous factors such as cell type (32), growth conditions (33,34), protein overexpression (35), and the detailed procedures used to isolate vesicles (36,37). This miscibility transition is not observed in intact cell membranes (38,39), possibly because direct or indirect coupling to internal structures such as the actin cortex precludes the formation of micron-sized domains (38–40). Nonetheless, it is often speculated that the value of T_{mix} predicts the magnitude of lipid-mediated heterogeneity in the intact cells from which the vesicles were derived, with higher GPMV transition temperatures predicting more robust heterogeneity in live cells at

Submitted March 3, 2017, and accepted for publication April 5, 2017.
*Correspondence: sveatch@umich.edu
Editor: Anne Kenworthy.
http://dx.doi.org/10.1016/j.bpj.2017.04.052

fixed growth temperature (41). In this study, we explore how plasma membrane T_{mix} varies with growth temperatures in a zebrafish cell line that can be adapted to grow over a range of temperatures.

MATERIALS AND METHODS

Cell culture

Zebrafish (ZF4) cells (42) were obtained from John Kuwada at the University of Michigan. Cells were cultured in medium containing 445 mL DMEM/F12, 50 mL 10% HI-FBS, and 5 mL 1% Pen-Strep in 5% CO_2. Optimal growth temperature is 28°C. ZF4 cells were grown at 20, 24, 28, and 32°C. All cell culture reagents were purchased from Thermo Fisher Scientific (Waltham, MA) unless otherwise indicated. All other reagents were purchased from Sigma-Aldrich (St. Louis, MO) unless otherwise indicated.

Preparation of GPMVs

GPMVs were isolated from ZF4 cells following established protocols (37,43) with the following minor modifications. For imaging studies, ZF4 cells were labeled with 2 μg/mL DiI-C_{12} (Thermo Fisher Scientific) in a 1% methanol solution for 10 min. Cells were then incubated for at least 1 h while gently shaking with a vesiculation buffer consisting of 100 μM $CaCl_2$, 500 μM HEPES, 7.5 mM NaCl, 25 mM formaldehyde, and 2 mM dithiothreitol (DTT) at pH 7.4. GPMVs spontaneously released from cells were typically imaged immediately after harvesting.

For lipidomics analysis, unlabeled ZF4 cells were incubated for 1 h while gently shaking in 100 μM $CaCl_2$, 500 μM HEPES, 7.5 mM NaCl, 25 mM formaldehyde, and 2 mM *n*-ethylmaleimide (NEM). NEM was used for lipidomic studies instead of DTT because previous work has shown that a combination of paraformaldehyde and DTT leads to chemical cross linking between phosphatidylethanolamine (PE) lipids and membrane proteins (36). Such covalent cross links prevent PE from being extracted into the organic phase during the Folch extraction, and therefore these lipids are not detected in lipidomics measurements. NEM only modifies terminal sulfhydryls, which are not present in any mammalian lipids, thus this isolation protocol is more appropriate for lipidomics. GPMVs produced using NEM tend to have much lower (10–20°C) transition temperatures (36,37), making them inconvenient for T_{mix} measurements. Extracted GPMVs were concentrated through centrifugation and submitted for lipidomic analysis without further purification. Centrifugation included one short, low-speed spin to pellet any whole cells followed by a longer high-speed spin to pellet the GPMVs. The pellet was washed once with ammonium bicarbonate buffer and was resuspended in a small volume of ammonium bicarbonate buffer. Total protein was quantified using a BCA assay (Thermo Fisher Scientific).

Time series measurements

ZF4 cells adapted for growth at 28°C were plated into multiple identical dishes and incubated overnight at 28°C to allow for cells to become adherent. Cells were moved to a 20°C incubator the next morning. Dishes were extracted for GPMV isolation on that first day (day 0) and on subsequent days at the same time. In the majority of time-series experiments, identical dishes were plated to probe cellular proliferation by cell counting. Cells were lifted in 0.25% trypsin EDTA, and counted using a Reichert Bright-Line hemocytometer (Thermo Fisher Scientific).

Imaging

GPMVs were imaged between coverslips on a home-built Peltier temperature stage on an inverted epifluorescence microscope (IX81; Olympus, Center Valley, PA) using a 40×, 0.95 NA air objective and a Cy3 filter-set (Chroma Technology, Bellows Falls, CT). A Peltier device (Custom Thermoelectric, Bishopville, MD) was thermally connected to the sample whose temperature was controlled by a PID-type controller unit from Oven Industries (Camp Hill, PA) and a water-circulating heat sink (Custom Thermoelectric). Images of fields of vesicles were acquired using a Neo SCMOS camera (Andor, South Windsor, CT) while the stage was maintained at constant temperature.

In postprocessing, vesicles within images were manually assigned to contain either a single phase or two coexisting phases, and vesicles were counted using custom software written in the software MATLAB (The MathWorks, Natick, MA). This information was used to construct a plot showing how the fraction of phase-separated vesicles varies with temperature. These points were fit to a sigmoidal function to extract the midpoint of the transition (T_{mix}), which is the temperature where 50% of GPMVs contained coexisting phases, as follows:

$$\%\ \text{separated} = 100 \times \left(1 - \frac{1}{1 + e^{-(T - T_{mix})/B}}\right).$$

The parameter B describes the slope of the sigmoid function and was not used in further analysis.

Analysis of lipidomics data

ZF4 lipidomes were processed from concentrated GPMV samples by Lipotype (Dresden, Germany) using mass spectrometry, which probed for >1000 distinct lipid species. Briefly, lipidomes were obtained by extracting concentrated GPMV samples in the presence of lipid class-specific standards, then acquiring mass spectra on a Q Exactive Hybrid Quadrupole-Orbitrap Mass Spectrometer (Thermo Fisher Scientific) equipped with an automated nanoflow electrospray ion source in both positive and negative ion mode. Lipids were identified using LipotypeXplorer (44) and after normalizing to standards, values reported have units of pmol. More extensive experimental methods can be found elsewhere (34,45,46).

Glycerophospholipids (GPLs) were identified by their headgroups (e.g., phosphatidylcholine (PC)), linkages (e.g. PC versus plasmologen PC), the number of hydroxyls, and the length (number of carbons) and level of unsaturation (number of double bonds) of each of their sn-1 and sn-2 fatty acid (FA) chains. For sphingomyelin (SM), the lipidomics analysis reported on the number of carbons and double bonds in the sphingosine and FA chains combined.

When lipids were grouped by headgroup type, we report the mol % of the headgroup normalized by total lipid including cholesterol. When lipids were grouped by lipid unsaturation, we report the mol % of the presence of the specific unsaturation value normalized by total lipid excluding cholesterol. When FAs were grouped by unsaturation or chain length, we only report FA from GPL and values are normalized to total moles of FA within GPL (twice the moles of GPL). We also conducted the FA analysis including FA within SM lipids, but results do not differ significantly due to the small mol % of SM in the lipidome as a whole.

All data analysis was carried out in the software MATLAB (The MathWorks, Natick, MA).

RESULTS

GPMV T_{mix} varies with growth temperatures in the ZF4 cell line

The ZF4 cell line is a fibroblast-like cell line isolated from zebrafish embryos that can be adapted to grow over a range of temperatures (42). In a first set of experiments, ZF4 cells were grown at temperatures between 20 and 32°C for at

least one week before fluorescent labeling and GPMV isolation as described in Materials and Methods. GPMV T_{mix} was then measured by monitoring the lateral distribution of the liquid-disordered phase marker DiI-C_{12} within fluorescence images of distinct fields of vesicles acquired over a range of temperatures, as illustrated in Fig. 1, *A* and *B*. Images are used to tabulate the fraction of vesicles that contain two coexisting liquid phases at different temperatures. T_{mix} is defined as the interpolated temperature where 50% of vesicles have undergone the miscibility transition, which is the average transition temperature of the sample.

As in previous studies, we find that the width of the miscibility transition measured over a population of vesicles (5–15°C) is much broader than the width of the transition in a single vesicle (<1°C), and that there is significant day-to-day variation in the measured value of T_{mix} (Fig. 1 *B*) (29,43). Past work in another cell type found that GPMV transition temperatures are sensitive to the local surface density of the cells from which they were derived (33). We hypothesize that the heterogeneity in T_{mix} observed here reflects variations in local density within a single dish and variation in average density in dishes examined on different days, because these parameters were not specifically controlled in these measurements.

Fig. 1 *C* shows data used to determine T_{mix} from cells grown on different days and at different adapted growth temperatures, revealing a clear trend toward lower transition temperatures at lower growth temperatures. Fig. 1 *D* shows the average values obtained for T_{mix} at each growth temperature. These points are well fit to a line of slope one (1.1 ± 0.1), indicating that T_{mix}, on average, remains a fixed number of degrees below the adapted growth temperature for all growth temperatures examined. This fixed temperature difference is 16.7 ± 1.2°C for the four growth temperatures examined, where the error indicates the standard deviation over the four measurements. Interestingly, values for T_{mix} measured from cells adapted for growth at 20°C fell systematically below the linear fit. One possible explanation for this discrepancy is that cells are not able to fully adapt to growth at this temperature, as past reports only examined cells adapted for growth at 22°C (42). Consistent with this idea, we found that cells occasionally experienced growth arrest when held at 20°C for extended times.

Overall, the results presented in Fig. 1 indicate that ZF4 cells adapted to grow at different temperatures produce GPMVs with average miscibility transition temperatures roughly 17°C below respective growth temperatures. This finding suggests that ZF4 cells actively tune their membrane composition to maintain this average temperature difference. An alternative explanation is that the cell tunes its membrane composition to maintain some other membrane property that is well correlated with T_{mix}.

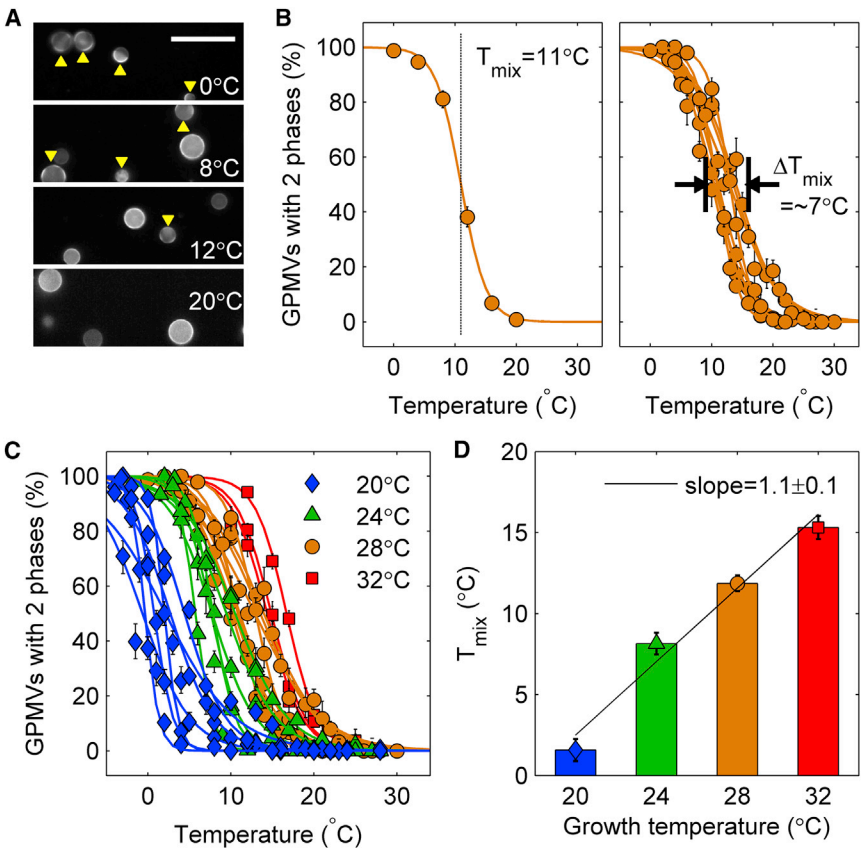

FIGURE 1 GPMV transition temperatures shift with growth temperatures in the ZF4 cell line. (*A*) Shown here are representative fields of DiI-C_{12} labeled GPMVs isolated from ZF4 cells adapted for growth at 28°C and imaged at different temperatures. The fluorophore partitions strongly into the liquid-disordered phase, and phase-separated vesicles are identified by monitoring the lateral distribution of this probe. Phase-separated GPMVs are indicated with yellow arrows and the scale bar represents 50 μm. (*B*) (*Left*) Multiple images like the ones shown in (*A*) are acquired at several fixed temperatures and are used to tabulate the percentage of GPMVs that contain coexisting liquid phases as a function of temperature. These curves are fit to a sigmoid function to extract the midpoint of the transition within the sample, defining T_{mix}. (*Right*) Curves from cells grown at 28°C but isolated on different days. These show systematic differences in the fraction of phase-separated vesicles as a function of temperature. This manifests itself as T_{mix} having some day-to-day variation, which in this example spans roughly 7°C. (*C*) Shown here are curves like those shown in (*B*) but generated from GPMVs from cells adapted for growth at different temperatures as indicated in the legend. (*D*) Shown here are average values of GPMV T_{mix} plotted as a function of growth temperature. The fit is to a line with a slope of 1.1 ± 0.1°C. The same symbols and colors are used to depict growth temperatures in (*B*)–(*D*). To see this figure in color, go online.

GPMVs from ZF4 cells exhibit composition fluctuations and modulated domains

Past work in GPMVs isolated from mammalian cells has shown that GPMVs can exhibit critical phase behavior (29). This is evidenced by micron sized composition fluctuations on the vesicle surface at temperatures slightly above the miscibility transition, and undulating domain boundaries in vesicles viewed at temperatures slightly below the miscibility transition. We observe evidence for similar composition fluctuations in GPMVs isolated from ZF4 cells, as indicated in Fig. 2.

Previous work has also reported evidence for modulated phases in model membranes of purified components (47,48). In this past work, domains tend to be arranged in a regular pattern on the vesicle surface, or alternately domains arrange in parallel stripes with occasional defects. Vesicles exhibiting these types of behaviors are also observed in GPMVs isolated from ZF4 cells.

Vesicles containing fluctuations, modulated domains, and complete phase separation can be detected within the same preparation of GPMVs. These behaviors can also be observed within the same GPMV, as shown in Fig. 2 *B* and Movie S1. At high temperature, this vesicle appears to contain micronscale composition fluctuations on the vesicle surface. As temperature is lowered, fluctuations become stripes with well-defined widths but fluctuating boundaries. As temperature is lowered further, stripes become thicker and domain boundaries become less rough. At the lowest temperature imaged, phase-separated domains in this vesicle take on a more conventional appearance, with large circular domains as well as smaller domains that appear to not have coarsened fully. This vesicle represents an example of a possible behavior of ZF4 GPMVs and is not representative of all vesicles. Also, these behaviors are likely not a specific consequence of being derived from ZF4 cells. Further experiments and analysis would be required to better understand the physical origins of the observed behaviors.

Adaptation of GPMV T_{mix} occurs over approximately one cell cycle

To explore the dynamics of T_{mix} adaptation, ZF4 cells adapted for growth at 28°C were transferred to a 20°C incubator and GPMVs were prepared for measurements of T_{mix} over multiple subsequent days. The result of a representative time-course measurement is shown in Fig. 3, *A* and *B*, and an average curve containing four distinct experiments is shown in Fig. 3 *C*. T_{mix} drops sharply within three days of incubation at 20°C, followed by a plateau that extends up to a week. We fit these data to the exponential decay, $T_{mix}(t) = T_{mix20} + \Delta T_{mix} \times \exp(-t/\tau)$, to estimate a time-constant of this adaptation of $\tau = 1.3 \pm 0.5$ days. Consistent with data presented in Fig. 1 *D*, the magnitude in the drop of T_{mix} ($\Delta T_{mix} = 10.8 \pm 1.7$°C) marginally exceeds the temperature difference in growth temperature (8°C).

Fig. 3 *D* shows how cell numbers increase over time in this measurement. For three of the four experiments included in Fig. 3 *C*, identical dishes were prepared for an experiment to measure cell expansion under the same growth conditions. Fig. 3 *D* shows the number of cells present within dishes as a function of time after moving cells to 20°C. We find that the time taken to adjust T_{mix} ($\tau = 1.3 \pm 0.5$) is in reasonable agreement with the doubling time of cells under these growth conditions (1.7 ± 0.1 days). This timing suggests that cells may adapt T_{mix} through alterations of their membrane composition through the normal lipid and protein synthesis pathways that occur within the cell cycle. We also note that growth appears linear in time, which is different from the exponential growth typically observed for cells in culture. This could be a result of cellular adaptation to the lower growth

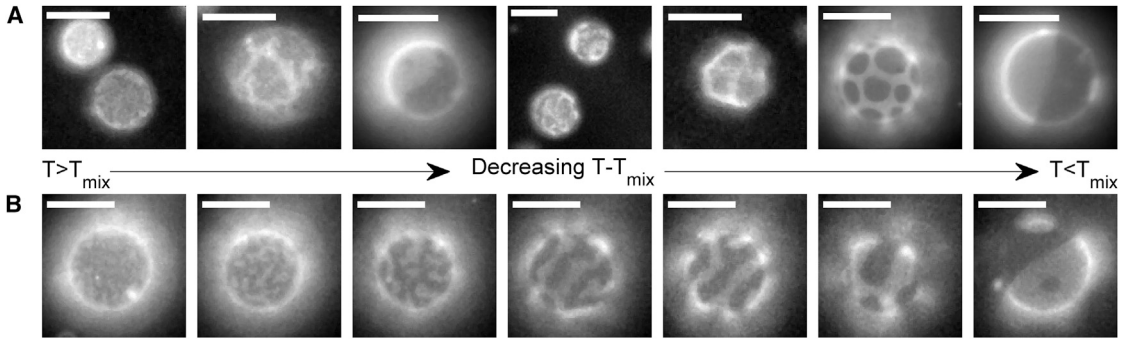

FIGURE 2 Images of ZF4-derived GMPVs. (*A*) Shown here are representative GPMVs displaying different domain morphologies. Domains, when present, are more likely to have rough and fluctuating boundaries when temperature is above or close to the miscibility transition temperature for the specific vesicle (T_{mix}). At lower temperatures, sometimes domains fully coarsen so that each phase takes up a hemisphere of the vesicle. In other cases, domains form stable and regular circular or striped regions characteristic of modulated domains. (*B*) Shown here are images of a single vesicle imaged over a range of temperatures. Temperature was not carefully monitored in this example, but was varied from above T_{mix} (*far left*) to below T_{mix} (*far right*). These images are captured from frames within Movie S1. The scale bar represents 10 μm. To see this figure in color, go online.

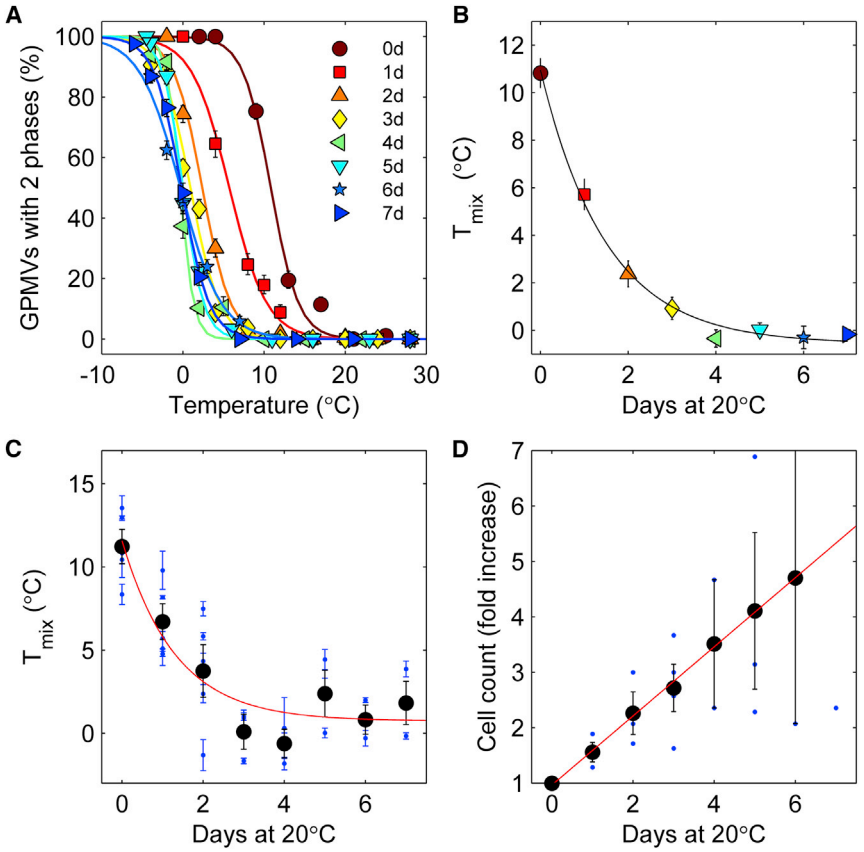

FIGURE 3 GPMV transition temperatures adapt to a temperature jump in roughly the same time it takes for cells to double. (*A* and *B*) Given here is a representative time-course experiment for cells adapted for growth and plated at 28°C before being moved to a 20°C incubator on day 0 (0 day). Raw curves showing the fraction of vesicles containing two liquid phases are shown in (*A*) and are used to determine the average values plotted in (*B*), with the symbols consistent between the two panels. (*C*) Given here is the variation in T_{mix} as a function of days in culture averaged over four distinct measurements, including the one shown in (*A*) and (*B*). Points are fit to an exponential decay, $T_{mix}(t) = T_{mix20} + \Delta T_{mix} \times \exp(-t/\tau)$, with $T_{mix20} = 0.7 \pm 1.0$°C, $\Delta T_{mix} = 10.8 \pm 1.7$°C, and $\tau = 1.3 \pm 0.5$ days. (*D*) For three of the measurements shown in (*C*), we also counted cells in dishes prepared identically to the ones used for GPMV isolation. We observed a roughly linear increase in the number of cells with increasing time, with the time required for doubling of 1.7 ± 0.2 days. Errors in parameter values reported for (*C*) and (*D*) are 68% confidence interval estimates evaluated from the fitting procedure. To see this figure in color, go online.

temperature, or due to the inability of these cells to fully adapt to growth at 20°C.

ZF4 cells adapted for growth at different temperatures have different lipid compositions

Because GPMVs are examined in isolation, the differences in transition temperatures observed for GPMVs harvested from cells grown at 20 and 28°C must be a consequence of their having different membrane compositions. In principle, these vesicles could be made up of different lipids or different ratios of the same lipids, contain different proteins or expression levels of proteins, different concentrations of other membrane soluble small molecules, or any combination of these variations. Hypothesizing that the comprehensive lipid composition is a major driver of membrane biophysical properties, we examined the lipidomes of GPMVs isolated from ZF4 cells adapted for growth at either 20 or 28°C, and results are summarized in Fig. 4.

ZF4-derived GPMVs contain a wide assortment of different lipid species. Fourteen distinct lipids are present at a level of 1 mol % or more, and >100 lipids are present at a level of 0.1% or more. The lipidomes of GPMVs isolated from cells grown at 20 and 28°C are more alike than they are different, with average values over all GPMVs harvested from cells grown at both temperatures shown in Fig. 4, *A–C*. When lipidomes are grouped by lipid headgroup type (Fig. 4 *A*), they both contain high molar fractions of cholesterol and PC lipids. After PC, the second most abundant phospholipid is plasmologen PE, which is present at 8.3 mol % on average. Plasmologens are a type of ether PC or PE that contain a vinyl ether linkage at the sn-1 position, an ester linkage at the sn-2 position, and have not been widely studied in model membrane experiments. When grouped by total lipid unsaturation (Fig. 4 *B*), <2.5 mol % of lipids are either fully saturated phospholipids or sphingomyelin and >40% contain at least three unsaturated bonds. When examined as individual FAs (Fig. 4 *C*), polyunsaturated FAs (PUFAs) or FAs that contain at least two unsaturated bonds comprise >25% of all lipid incorporated FA. When examined in the context of FA length, the most abundant FA length in both samples is 18 carbons, with the average length being just under this value. Consistent with previous studies (32,34), these lipidomes do not closely resemble the model membranes typically used to study liquid immiscibility which typically are composed of roughly equal molar fractions of fully saturated lipids, monounsaturated lipids, and cholesterol (41,49).

Despite their broad similarity, there are some notable differences between the lipidomes of GPMVs from cells grown

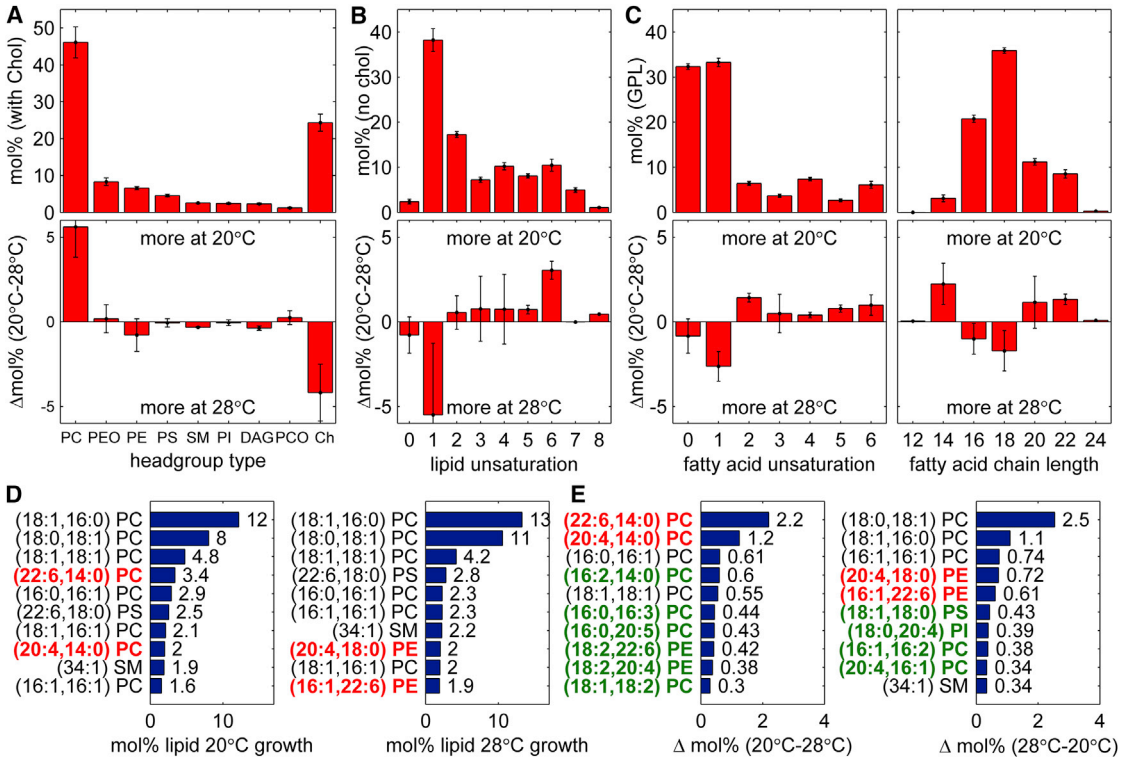

FIGURE 4 Summary of lipidomics results for GPMVs isolated from ZF4 adapted for growth at 20 and 28°C. (*A–C*) Given here is the molar percent of lipid types grouped according to headgroup type, total lipid unsaturation, individual fatty acid chain unsaturation, and fatty acid chain length. Top panels indicate average values acquired for samples isolated from cells grown at both 20 and 28°C, and error bars indicate the mean ± SE over four measurements. Bottom panels indicate the mol % change observed for samples grown at 20 and 28°C, and error bars indicate the mean ± SE over two difference measurements. (*D*) Given here are the 10 most abundant lipids observed in GPMVs from cells grown at 20°C (*left*) and 28°C (*right*). Lipid species not present on both lists are indicated in red text. (*E*) Shown here are the 10 lipids found at higher abundance in GPMVs from cells grown at 20 vs. 28°C (*left*) or 28 vs. 20°C, in order of the magnitude of their increased abundance. Lipids indicated in red text are repeated from (*D*). Lipid species not present in either list in (*D*) are indicated as green text. To see this figure in color, go online.

at 20 and 28°C. As shown in Fig. 4 *A*, cells grown at the lower temperature produce GPMVs with more PC lipids and less cholesterol than GPMVs from cells grown at the elevated temperature. Cells grown at the lower temperature also produce GPMVs with more PUFA and less monounsaturated FA chains than GPMVs from higher temperature cells. Interestingly, GPMVs from cells grown at 20°C have a broader distribution of fatty acid chain lengths although retaining the same average value. Due to the variation observed in our biological replicates along with the small number of samples investigated (two at each temperature), it is difficult to draw significance from the changes of any specific parameter, although the general trends observed here are consistent with reports in the literature describing fish lipids from animals adapted for growth at different temperatures (4–6,50–52).

We also examined the individual lipid species that are most abundant in GPMVs, and whose levels vary the most between GPMVs isolated from cells grown at different temperatures (Fig. 4, *D* and *E*). For both growth temperatures, cholesterol is excluded from the list for clarity but is by far the most abundant lipid, averaging 22 ± 4% in cells grown at 20°C and 26 ± 3% in cells grown at 28°C, where errors are the mean ± SE over two measurements. At both growth temperatures, the three next most abundant lipids contain the PC headgroup and either saturated or mono-unsaturated fatty acid chains. Together these lipids make up close to 25% of the total noncholesterol lipid (24.8% at 20°C and 28.2% at 28°C). Of the remaining six most abundant lipids, four are among abundant lipids in GPMVs from both 20 and 28°C grown cells. The exceptions are two PUFA PC lipids present at high abundance in GPMVs from cells grown at 20°C, and two PUFA PE lipids found in GPMVs from cells grown at 28°C. Not surprisingly, these same two lipid pairs are present in the list of lipid species that experience the largest changes in concentrations in GPMVs from the two temperature conditions.

We also note that both lipids present in high abundance at 20°C and not at high abundance at 28°C contain a fully saturated sn-2 chain (*red text* within *left panel* of Fig. 4, *D* and *E*). In both cases, these are coupled to a longer PUFA (22:6 and 20:4) at the sn-1 position. Along these lines, we generally find that GPMVs made from 20°C adapted cells contain

4.5 ± 2 mol % more lipids with one highly unsaturated chain (≥4 unsaturations) attached to a fully saturated chain than those isolated from cells grown at 28°C.

DISCUSSION

In this study we demonstrate that GPMVs isolated from ZF4 cells alter their plasma membrane composition in a way that shifts GPMV transition temperatures as cells adapt to growth at different temperatures. Specifically, T_{mix} in adapted cells is found to be roughly 17°C below growth temperature across a range of growth temperatures. When cells are subjected to an 8°C temperature drop, they take several days to adapt their T_{mix}, comparable to the doubling time of these cells under this growth condition. Finally, we have analyzed the lipid composition of GPMVs isolated from ZF4 cells grown at 20 and 28°C. Although the lipid content of these vesicles is broadly similar, cells grown at 20°C produce GPMVs with less cholesterol, more PUFAs, and more highly asymmetric lipids containing one highly unsaturated and one mostly unsaturated acyl chain.

The above observations do not discern whether cells sense and maintain T_{mix} to a specified level below growth temperature, or alternatively, if the changes in T_{mix} are a consequence of cellular membrane tuning to maintain some other property such as viscosity, water permeability, or membrane stiffness. Past work in fish and other organisms has argued that adaptation of membrane lipids to temperature changes is primarily to maintain membrane viscosity and ion permeability within an acceptable range for biological functions (6,8,21,22,24,50–52). Based on this extensive past work, we anticipate that measurements of average membrane order, which often serve as a proxy for membrane viscosity, would also maintain roughly constant values at different adapted growth temperatures in ZF4 cells. For example, the observed decreases in cholesterol and increases in PUFAs in cells grown at lower temperature are in line with this past work. The changes in levels of these components are expected to produce membranes with decreased chain order and increased lateral mobility that will counteract the effect of lowering temperature on these two properties. We note that the addition of highly disordered components alone, including PUFA lipids or detergents, tend to raise miscibility transition temperatures or expand the miscibility gap in membranes probed at constant temperature (53–55), because these components partition strongly into liquid-disordered domains in membranes (56). Also, reduction of cholesterol in model membranes of purified components also tends to raise transition temperatures (49). Our observation that transition temperatures are instead depressed in membranes with less cholesterol and more highly disordered PUFA chains suggests that cells are adjusting additional factors to tune both viscosity and T_{mix} simultaneously. It is possible that one reason for the vast diversity of lipids found in plasma membranes is to enable cells to tune many physical and biological properties within the same membrane.

Our experiments indicate that $T - T_{mix}$ remains roughly constant on average when cells are adapted to grow at different ambient temperatures. Here we find that $T - T_{mix}$ ~17°C, although it is important to note that the absolute value of GPMV transition temperature depends on the method by which they are prepared (37). The method employed in this study for T_{mix} determination, namely incubation of cells with DTT, tends to produce GPMVs with higher T_{mix} than those produced with other reducing agents or vesiculation procedures. In light of this, it is likely that the GPMV transition temperatures observed here are elevated compared to that of the intact plasma membranes from which they are derived. Nonetheless, we anticipate that the actions of DTT should be consistent across growth conditions. Unfortunately, this cannot be tested directly because the transition temperatures observed are already close to the lower end of our detection limit for some growth temperatures. If the GPMV preparation procedure employed here artificially raises transition temperatures by 15°C, which is an upper estimate based on our experience and evidence in Levental et al. (36), then $T - T_{mix}$ ~32°C.

In addition to the observed miscibility transition, ZF4-derived GPMVs also appear to have membrane compositions that are close to critical compositions. Similar to GPMVs isolated from other cell types, ZF4-derived GPMVs are uniform at high temperature, contain roughly equal surface fractions of liquid-ordered and liquid-disordered phases at low temperature, and contain extended domains with fluctuating boundaries at temperatures close to T_{mix}. These observations suggest that ZF4 GPMVs reside near a critical point at the miscibility transition temperature, and because of this T_{mix} is also the critical temperature or T_C. In critical systems, physical properties including the compositional susceptibility, the average domain size, and the average domain lifetime depend strongly on the reduced temperature (t), or the normalized temperature difference between ambient temperature (T) and T_C in units of Kelvin ($t = (T - T_C)/T_C$) (29,57,58). It is possible that cells actively maintain a specific temperature difference between T_{mix} and growth temperatures to tune one or more of the related physical properties that depend on t. When $T - T_C = 17$°C, then $t = 0.06$, or growth temperature is 6% away from the critical temperature. This value of t predicts that membranes contain domains with a characteristic size of close to 20 nm at growth temperature (29,58). If instead $T - T_C$ is 32°C, then $t = 0.12$, and this increased value of t predicts that membranes contain domains with a characteristic size close to 10 nm at growth temperature.

Our experimental findings beg the question of why cells might tune the T_{mix} of their plasma membrane to be a specific temperature below growth temperature, and currently we can only speculate on possible explanations. One possibility, as suggested above, could be to enable equilibrium

domain structures with dimensions of 10–20 nm under growth conditions. This domain size could be generally useful to cells for controlling plasma membrane organization because it is larger than the size of individual lipids and proteins (0.5 to several nm) but smaller than the length-scale of cytoskeletal networks proximal to the membrane plane (50–400 nm) (38,59,60). Another possible reason for adjusting T_{mix} to a specific value below growth temperature could be to control how membrane domains extend or become stabilized when subsets of membrane components are organized through interactions outside of the membrane plane, as has been observed experimentally in both model membranes and intact cells (61,62). We have previously argued that this increased compositional susceptibility of critical membranes may contribute to the activation or modulation of signaling pathways initiated by receptor clustering (62,63). It is also possible that cells tune T_{mix} to adjust the magnitude of lipid domain-mediated interactions between proteins, which tend to attract proteins that prefer similar local lipid environments and repel proteins that prefer alternate local lipid environments (64,65), or to optimize the functional states of certain embedded proteins (66,67). Another consideration is that we observe a 5–15°C spread in T_{mix} from individual GPMVs adapted for growth at constant temperature, so cells apparently can adjust $T - T_{mix}$ to be within a broad range of values even under a single growth condition. It is possible that cells tune the average value of T_{mix} to be a fairly large distance below growth temperatures to give individual cells broad flexibility in adjusting their membrane composition to accomplish specific objectives while remaining in a one-phase region. Future work is needed to explore whether and how cells exploit these or other proposed consequences of a nearby miscibility transition to accomplish biological functions.

It is not obvious how to relate changes in GPMV lipid composition to the observed changes in T_{mix}. The overall lipid contents of GPMVs isolated from cells grown at different temperatures are broadly similar; however, some clear growth temperature-dependence was observable. Unfortunately, the currently limited understanding of the relationships between the complex composition of lipidomes and membrane biophysical properties prevents straightforward interpretation of how the observed lipidomic changes result in changes to T_{mix}. As mentioned above, raising cholesterol content tends to lower miscibility phase transition temperatures in three-component model membranes (49). Here we observe the reverse; we detect more cholesterol in GPMVs isolated from cells grown at a 28°C than in GPMVs from cells grown at 20°C, even though GPMVs from cells grown at 28°C have much higher transition temperatures. Past work in model membranes and GPMVs isolated from other cell types indicates that transition temperatures tend to be higher when membranes contain more highly unsaturated PUFA acyl chains (34,68). Here again, we observe the reverse; more PUFA lipids are found in GPMVs isolated from cells grown at 20°C than in GPMVs isolated from cells grown at 28°C, although the former have lower transition temperatures.

One observation that appears to be consistent with past work in model membranes is that the abundance of asymmetric hybrid lipids appears to inversely correlate with miscibility transition temperatures. Here, we find more highly asymmetric lipids in GPMVs with lower transition temperatures, and model membrane studies show that introducing the asymmetric lipids (16:0/18:1)PC (POPC) or (18:0/18:1)PC (SOPC) into ternary mixtures of (18:1/18:1) PC (DOPC), (16:0/16:0)PC (DPPC) and cholesterol or DOPC, (18:0/18:0)PC (DSPC) and cholesterol act to lower macroscopic phase transition temperatures or decrease the fraction of composition space where macroscopic phase coexistence is observed at constant temperature (47,48,69). It is possible that these lipids act as two-dimensional surfactants to reduce the interfacial energy between domains, favoring a mixed state and therefore lowering T_{mix} (56,70). It is also possible that these hybrid lipids more simply have physical properties that are intermediate to less asymmetric lipids typically found in either low temperature phase. This type of component is also expected to favor a mixed state and reduce T_{mix} (56). GPMVs contain many more unsaturated lipids than are typically found in purified model membranes that exhibit a miscibility transition, and the level of unsaturation of lipids found in coexisting phases must also dramatically differ between the two systems. It is possible that the asymmetric lipid 22:6/14:0 PC behaves similarly in a GPMV as the hybrid lipid 16:0/18:1 PC behaves in a model membrane of DOPC, DPPC, and cholesterol. We also note that some abundant PUFA lipids from cells grown at 28°C have PE headgroups in GPMVs, whereas the most abundant PUFA lipids from cells grown at 20°C have PC headgroups. PE lipids have been shown to have weaker or more repulsive interactions with cholesterol in model membranes, especially when conjugated to PUFA chains (71,72), and this could further impact miscibility phase transition temperatures.

Finally, it is possible that changes in T_{mix} result from changes in the concentration or type of nonlipid membrane components. These could include proteins, peptides, and nonlipid membrane-soluble small molecules. Past work has shown that GPMV transition temperatures can depend on the transient expression of membrane proteins (35), and can be dramatically altered by small molecules such as *n*-alcohols (43,67) and detergents (53,54). These and other similar molecules would not be detected in this study.

CONCLUSIONS

We find that GPMV miscibility transition temperatures scale simply with the growth temperature of the ZF4 cells from which they were derived. Our observations are that ZF4 cells maintain their plasma membrane transition

temperature to be roughly 17°C below growth temperature on average, and that cells fully adapt their GPMV transition temperature over roughly two days when growth temperature is lowered by 8°C. ZF4 cells grown at different temperatures produce GPMVs with slightly different lipidomes. Namely, cells grown at lower temperature produce GPMVs with lower levels of cholesterol and increased levels of lipids with polyunsaturated chains. Further work is needed to identify how changes in lipid composition of the membrane directly lead to changes in T_{mix}, or if changes in T_{mix} are due to additional nonlipid membrane constituents. Finally, although it is possible that changes in T_{mix} occur due to cellular tuning of other membrane properties, the experimental observation that T_{mix} is maintained at a set temperature differential below growth temperature is consistent with the hypothesis that cells tune their membrane compositions to maintain a desired distance from the miscibility transition. The added observation that GPMVs appear to have critical compositions supports the idea that cells tune plasma membrane composition to exploit the unique physical properties present in supercritical systems to accomplish biological functions.

SUPPORTING MATERIAL

One movie is available at http://www.biophysj.org/biophysj/supplemental/S0006-3495(17)30505-2.

AUTHOR CONTRIBUTIONS

ZF4 cells were maintained by J.W. and K.W. GPMV transition temperature measurements were carried out by M.B. and J.W., and were analyzed by S.L.V. Cell counting experiments were carried out by M.B. and analyzed by S.L.V. Samples for lipidomic analysis were prepared by K.W. and lipidomes were analyzed by I.L. and S.L.V. The research was designed by S.L.V. and the paper was written by M.B., I.L., and S.L.V.

ACKNOWLEDGMENTS

We thank John Kuwada for providing ZF4 cells, Kaleab Mamo for assistance with early experiments, and Sarah Shelby for comments on the manuscript draft.

Research was funded by the National Science Foundation (NSF) (MCB 1552439 to S.L.V.), the National Institutes of Health (NIH) (R01 GM110052 to S.L.V. and R01 GM114282 to I.L.), and the Cancer Prevention and Research Institute of Texas (R1215 to I.L.).

REFERENCES

1. Hunter, K., and A. H. Rose. 1972. Lipid composition of *Saccharomyces cerevisiae* as influenced by growth temperature. *Biochim. Biophys. Acta.* 260:639–653.
2. Farrell, J., and A. Rose. 1967. Temperature effects on microorganisms. *Annu. Rev. Microbiol.* 21:101–120.
3. Kates, M., and R. M. Baxter. 1962. Lipid composition of mesophilic and psychrophilic yeasts (Candida species) as influenced by environmental temperature. *Can. J. Biochem. Physiol.* 40:1213–1227.
4. Anderson, T. R. 1970. Temperature adaptation and the phospholipids of membranes in goldfish (*Carassius auratus*). *Comp. Biochem. Physiol.* 33:663–687.
5. Dey, I., C. Buda, …, T. Farkas. 1993. Molecular and structural composition of phospholipid membranes in livers of marine and freshwater fish in relation to temperature. *Proc. Natl. Acad. Sci. USA.* 90:7498–7502.
6. Hazel, J. R., and E. Zerba. 1986. Adaptation of biological-membranes to temperature—molecular-species compositions of phosphatidylcholine and phosphatidylethanolamine in mitochondrial and microsomal-membranes of liver from thermally-acclimated rainbow-trout. *J. Comp. Physiol. B.* 156:665–674.
7. Roy, R., A. B. Das, and D. Ghosh. 1997. Regulation of membrane lipid bilayer structure during seasonal variation: a study on the brain membranes of *Clarias batrachus*. *Biochim. Biophys. Acta.* 1323:65–74.
8. Weaver, F. E., S. R. Shaikh, and M. Edidin. 2008. Plasma membrane lipid diffusion and composition of sea urchin egg membranes vary with ocean temperature. *Chem. Phys. Lipids.* 151:62–65.
9. Huffer, S., M. E. Clark, …, D. S. Clark. 2011. Role of alcohols in growth, lipid composition, and membrane fluidity of yeasts, bacteria, and archaea. *Appl. Environ. Microbiol.* 77:6400–6408.
10. You, K. M., C. L. Rosenfield, and D. C. Knipple. 2003. Ethanol tolerance in the yeast Saccharomyces cerevisiae is dependent on cellular oleic acid content. *Appl. Environ. Microbiol.* 69:1499–1503.
11. Alexandre, H., I. Rousseaux, and C. Charpentier. 1994. Ethanol adaptation mechanisms in *Saccharomyces cerevisiae*. *Biotechnol. Appl. Biochem.* 20:173–183.
12. Jackowski, S. 1996. Cell cycle regulation of membrane phospholipid metabolism. *J. Biol. Chem.* 271:20219–20222.
13. Spiegel, S., and A. H. Merrill, Jr. 1996. Sphingolipid metabolism and cell growth regulation. *FASEB J.* 10:1388–1397.
14. Koeberle, A., H. Shindou, …, O. Werz. 2013. Arachidonoyl-phosphatidylcholine oscillates during the cell cycle and counteracts proliferation by suppressing Akt membrane binding. *Proc. Natl. Acad. Sci. USA.* 110:2546–2551.
15. Atilla-Gokcumen, G. E., E. Muro, …, U. S. Eggert. 2014. Dividing cells regulate their lipid composition and localization. *Cell.* 156:428–439.
16. Ponec, M., A. Weerheim, …, D. H. Nugteren. 1988. Lipid composition of cultured human keratinocytes in relation to their differentiation. *J. Lipid Res.* 29:949–961.
17. Gulaya, N. M., G. L. Volkov, …, A. A. Melnik. 1989. Changes in lipid composition of neuroblastoma C1300 N18 cell during differentiation. *Neuroscience.* 30:153–164.
18. Santos, C. R., and A. Schulze. 2012. Lipid metabolism in cancer. *FEBS J.* 279:2610–2623.
19. Cutler, R. G., J. Kelly, …, M. P. Mattson. 2004. Involvement of oxidative stress-induced abnormalities in ceramide and cholesterol metabolism in brain aging and Alzheimer's disease. *Proc. Natl. Acad. Sci. USA.* 101:2070–2075.
20. Maes, M., R. Smith, …, H. Meltzer. 1996. Fatty acid composition in major depression: decreased omega-3 fractions in cholesteryl esters and increased C20:4 omega-6/C20:5 omega-3 ratio in cholesteryl esters and phospholipids. *J. Affect. Disord.* 38:35–46.
21. Hazel, J. R. 1995. Thermal adaptation in biological membranes: is homeoviscous adaptation the explanation? *Annu. Rev. Physiol.* 57:19–42.
22. Ernst, R., C. S. Ejsing, and B. Antonny. 2016. Homeoviscous adaptation and the regulation of membrane lipids. *J. Mol. Biol.* 428 (24 Pt A):4776–4791.
23. Covino, R., S. Ballweg, …, R. Ernst. 2016. A eukaryotic sensor for membrane lipid saturation. *Mol. Cell.* 63:49–59.
24. Williams, E., and G. Somero. 1996. Seasonal-, tidal-cycle- and microhabitat-related variation in membrane order of phospholipid vesicles from gills of the intertidal mussel *Mytilus californianus*. *J. Exp. Biol.* 199:1587–1596.

25. Jin, A. J., M. Edidin, …, N. L. Gershfeld. 1999. A singular state of membrane lipids at cell growth temperatures. *Biochemistry.* 38: 13275–13278.

26. Morein, S., A. Andersson, …, G. Lindblom. 1996. Wild-type *Escherichia coli* cells regulate the membrane lipid composition in a "window" between gel and non-lamellar structures. *J. Biol. Chem.* 271:6801–6809.

27. Osterberg, F., L. Rilfors, …, S. M. Gruner. 1995. Lipid extracts from membranes of *Acholeplasma laidlawii* A grown with different fatty acids have a nearly constant spontaneous curvature. *Biochim. Biophys. Acta.* 1257:18–24.

28. Simons, K., and E. Ikonen. 1997. Functional rafts in cell membranes. *Nature.* 387:569–572.

29. Veatch, S. L., P. Cicuta, …, B. Baird. 2008. Critical fluctuations in plasma membrane vesicles. *ACS Chem. Biol.* 3:287–293.

30. Lingwood, D., and K. Simons. 2010. Lipid rafts as a membrane-organizing principle. *Science.* 327:46–50.

31. Baumgart, T., A. T. Hammond, …, W. W. Webb. 2007. Large-scale fluid/fluid phase separation of proteins and lipids in giant plasma membrane vesicles. *Proc. Natl. Acad. Sci. USA.* 104:3165–3170.

32. Tulodziecka, K., B. B. Diaz-Rohrer, …, I. Levental. 2016. Remodeling of the postsynaptic plasma membrane during neural development. *Mol. Biol. Cell.* 27:3480–3489.

33. Gray, E. M., G. Díaz-Vázquez, and S. L. Veatch. 2015. Growth conditions and cell cycle phase modulate phase transition temperatures in RBL-2H3 derived plasma membrane vesicles. *PLoS One.* 10: e0137741.

34. Levental, K. R., J. H. Lorent, …, I. Levental. 2016. Polyunsaturated lipids regulate membrane domain stability by tuning membrane order. *Biophys. J.* 110:1800–1810.

35. Podkalicka, J., A. Biernatowska, …, A. F. Sikorski. 2015. MPP1 as a factor regulating phase separation in giant plasma membrane-derived vesicles. *Biophys. J.* 108:2201–2211.

36. Levental, I., M. Grzybek, and K. Simons. 2011. Raft domains of variable properties and compositions in plasma membrane vesicles. *Proc. Natl. Acad. Sci. USA.* 108:11411–11416.

37. Levental, K. R., and I. Levental. 2015. Isolation of giant plasma membrane vesicles for evaluation of plasma membrane structure and protein partitioning. *Methods Mol. Biol.* 1232:65–77.

38. Machta, B. B., S. Papanikolaou, …, S. L. Veatch. 2011. Minimal model of plasma membrane heterogeneity requires coupling cortical actin to criticality. *Biophys. J.* 100:1668–1677.

39. Lee, I. H., S. Saha, …, J. T. Groves. 2015. Live cell plasma membranes do not exhibit a miscibility phase transition over a wide range of temperatures. *J. Phys. Chem. B.* 119:4450–4459.

40. Honigmann, A., S. Sadeghi, …, R. Vink. 2014. A lipid bound actin meshwork organizes liquid phase separation in model membranes. *eLife.* 3:e01671.

41. Levental, I., and S. L. Veatch. 2016. The continuing mystery of lipid rafts. *J. Mol. Biol.* 428 (24 Pt A):4749–4764.

42. Driever, W., and Z. Rangini. 1993. Characterization of a cell line derived from zebrafish (*Brachydanio rerio*) embryos. *In Vitro Cell. Dev. Biol. Anim.* 29A:749–754.

43. Gray, E., J. Karslake, …, S. L. Veatch. 2013. Liquid general anesthetics lower critical temperatures in plasma membrane vesicles. *Biophys. J.* 105:2751–2759.

44. Herzog, R., D. Schwudke, …, A. Shevchenko. 2011. A novel informatics concept for high-throughput shotgun lipidomics based on the molecular fragmentation query language. *Genome Biol.* 12:R8.

45. Sampaio, J. L., M. J. Gerl, …, A. Shevchenko. 2011. Membrane lipidome of an epithelial cell line. *Proc. Natl. Acad. Sci. USA.* 108: 1903–1907.

46. Klose, C., M. A. Surma, and K. Simons. 2013. Organellar lipidomics—background and perspectives. *Curr. Opin. Cell Biol.* 25:406–413.

47. Konyakhina, T. M., S. L. Goh, …, G. W. Feigenson. 2011. Control of a nanoscopic-to-macroscopic transition: modulated phases in four-component DSPC/DOPC/POPC/Chol giant unilamellar vesicles. *Biophys. J.* 101:L8–L10.

48. Goh, S. L., J. J. Amazon, and G. W. Feigenson. 2013. Toward a better raft model: modulated phases in the four-component bilayer, DSPC/DOPC/POPC/CHOL. *Biophys. J.* 104:853–862.

49. Veatch, S. L., and S. L. Keller. 2005. Seeing spots: complex phase behavior in simple membranes. *Biochim. Biophys. Acta.* 1746:172–185.

50. Johnston, P. V., and B. I. Roots. 1964. Brain lipid fatty acids and temperature acclimation. *Comp. Biochem. Physiol.* 11:303–309.

51. Knipprath, W. G., and J. F. Mead. 1968. The effect of the environmental temperature on the fatty acid composition and on the in vivo incorporation of 1-^{14}C-acetate in goldfish (*Carassius auratus* L.). *Lipids.* 3:121–128.

52. Roots, B. I. 1968. Phospholipids of goldfish (*Carassius auratus* L.) brain: the influence of environmental temperature. *Comp. Biochem. Physiol.* 25:457–466.

53. Heerklotz, H. 2002. Triton promotes domain formation in lipid raft mixtures. *Biophys. J.* 83:2693–2701.

54. Zhou, Y., K. N. Maxwell, …, I. Levental. 2013. Bile acids modulate signaling by functional perturbation of plasma membrane domains. *J. Biol. Chem.* 288:35660–35670.

55. Shaikh, S. R., A. C. Dumaual, …, S. R. Wassall. 2004. Oleic and docosahexaenoic acid differentially phase separate from lipid raft molecules: a comparative NMR, DSC, AFM, and detergent extraction study. *Biophys. J.* 87:1752–1766.

56. Meerschaert, R. L., and C. V. Kelly. 2015. Trace membrane additives affect lipid phases with distinct mechanisms: a modified Ising model. *Eur. Biophys. J.* 44:227–233.

57. Honerkamp-Smith, A. R., B. B. Machta, and S. L. Keller. 2012. Experimental observations of dynamic critical phenomena in a lipid membrane. *Phys. Rev. Lett.* 108:265702.

58. Honerkamp-Smith, A. R., S. L. Veatch, and S. L. Keller. 2009. An introduction to critical points for biophysicists; observations of compositional heterogeneity in lipid membranes. *Biochim. Biophys. Acta.* 1788:53–63.

59. Murase, K., T. Fujiwara, …, A. Kusumi. 2004. Ultrafine membrane compartments for molecular diffusion as revealed by single molecule techniques. *Biophys. J.* 86:4075–4093.

60. Fujiwara, T. K., K. Iwasawa, …, A. Kusumi. 2016. Confined diffusion of transmembrane proteins and lipids induced by the same actin meshwork lining the plasma membrane. *Mol. Biol. Cell.* 27:1101–1119.

61. Zhao, J., J. Wu, and S. L. Veatch. 2013. Adhesion stabilizes robust lipid heterogeneity in supercritical membranes at physiological temperature. *Biophys. J.* 104:825–834.

62. Stone, M. B., S. A. Shelby, …, S. L. Veatch. 2017. Protein sorting by lipid phase-like domains supports emergent signaling function in B lymphocyte plasma membranes. *eLife.* 6:e19891.

63. Shelby, S. A., S. L. Veatch, …, B. A. Baird. 2016. Functional nanoscale coupling of Lyn kinase with IgE-FcεRI is restricted by the actin cytoskeleton in early antigen-stimulated signaling. *Mol. Biol. Cell.* 27:3645–3658.

64. Katira, S., K. K. Mandadapu, …, D. Chandler. 2016. Pre-transition effects mediate forces of assembly between transmembrane proteins. *eLife.* 5:e13150.

65. Machta, B. B., S. L. Veatch, and J. P. Sethna. 2012. Critical Casimir forces in cellular membranes. *Phys. Rev. Lett.* 109:138101.

66. Kimchi, O., S. L. Veatch, and B. B. Machta. 2016. Allosteric regulation by a critical membrane. *arXiv:1607.06836.*.

67. Machta, B. B., E. Gray, …, S. L. Veatch. 2016. Conditions that stabilize membrane domains also antagonize *n*-alcohol anesthesia. *Biophys. J.* 111:537–545.

68. Lin, X., J. H. Lorent, …, I. Levental. 2016. Domain stability in biomimetic membranes driven by lipid polyunsaturation. *J. Phys. Chem. B.* 120:11930–11941.

69. Veatch, S. L., and S. L. Keller. 2005. Miscibility phase diagrams of giant vesicles containing sphingomyelin. *Phys. Rev. Lett.* 94: 148101.

70. Palmieri, B., and S. A. Safran. 2013. Hybrid lipids increase the probability of fluctuating nanodomains in mixed membranes. *Langmuir.* 29:5246–5261.

71. Huster, D., K. Arnold, and K. Gawrisch. 1998. Influence of docosahexaenoic acid and cholesterol on lateral lipid organization in phospholipid mixtures. *Biochemistry.* 37:17299–17308.

72. Wassall, S. R., and W. Stillwell. 2009. Polyunsaturated fatty acid-cholesterol interactions: domain formation in membranes. *Biochim. Biophys. Acta.* 1788:24–32.